9-METER-LONG 3D ULTRASONIC OBJECTS DETECTION VIA PACKAGED LITHIUM-NIOBATE PMUTS

Yande Peng[1†], Hanxiao Liu[1†], Chun-Ming Chen[1†], Wei Yue[1], Megan Teng[1], Pei-Chi Tsao[1], Seiji Umezawa[2], Shinsuke Ikeuchi[2], Yasuhiro Aida[2], and Liwei Lin[1]

[1]Department of Mechanical Engineering, University of California, Berkeley, USA, and [2]Murata Manufacturing Co., Ltd., Japan

[†]Yande Peng, Hanxiao Liu and Chun-Ming Chen contributed equally to this work.

2024 IEEE 37th International Conference on Micro Electro Mechanical Systems (MEMS) | 979-8-3503-5792-9/24/$31.00 ©2024 IEEE | DOI: 10.1109/MEMS58180.2024.10439314

ABSTRACT

This paper reports a 9-meter-long ultrasonic 3D detector based on a packaged lithium niobate PMUTs (piezoelectric micromachined ultrasonic transducers). Compared with the state-of-the-art reports, three distinctive achievements have been demonstrated: (1) high uniformity and wide bandwidth PMUTs by optimized package designs for highly efficient ultrasonic energy transfer; (2) a long-range receiving beamforming detection scheme on a 4×4 PMUT array for up to 9 m detection rang - comparable to the longest reported range via PMUTs; and (3) 3D detection of multiple static/moving objects with the field of view exceeding 50°. As such, this device is valuable for various applications such as obstacle avoidance when both low power consumption and small form factor are desirable, including aerial drones.

KEYWORDS

PMUTs, 3D object detection, long range sensing, machine vision.

INTRODUCTION

Range sensing is an indispensable technology in machine vision where different types of sensors (radar, optical, ultrasonic etc.) are used to detect the location or presence of surrounding objects [1, 2]. While different scenarios may require various sensors metrics, in systems of poor visibility condition under limited power and size requirements, such as obstacle avoidance for aerial drones, ultrasonic sensing stands out when compared with other technologies due to its intrinsic advantages of low power consumption, small form factor, as well as low operation frequency [3].

Although conventional bulk ultrasonic transducers have been widely used in automotive and industrial applications, piezoelectric micromachined ultrasonic transducers (PMUTs) exhibit advantages over its bulk counterparts in terms of size, cost, as well as integration capabilities on silicon substrates [4]. Recently, the development of micromachining technology has attracted substantial research interests in PMUTs, leading to considerable improvements in their performances, such as the range sensing technology [5, 6]. A single range sensor with sensing distance up to 9 m has been demonstrated with integrated ASIC [7]. However, for more complicated 3D space detections, the state-of-the-art reported PMUTs system can only go up to ~2 m [8, 9]. Bottlenecks of technology development involve several aspects. For example, the low electro-mechanical coupling coefficient (k_t^2) and piezoelectric constant (e_{31}) of the current AlN PMUTs limit their output acoustic pressure. In addition, frequency mismatch arising from the fabrication nonuniformity also poses challenges, especially for low-frequency PMUTs with bandwidth of only less than ten kHz [9].

Here, we introduce a low-frequency 3D ultrasonic detector based on the lithium-niobate thin film material as illustrated in **Figure 1**. A well-designed acoustic package is employed to broaden the bandwidth of the PMUTs as well as to induce a second acoustic resonance by the package. The low operating frequency and large bandwidth contribute to reduced attenuation and more efficient energy transfer in air. Leveraging these features, our prototype detector, comprising a 4×4 PMUTs array, manages to detect objects up to 9 m away with a field of view exceeding 50°. Furthermore, we demonstrate both static and moving object detections by using a receiving beamforming scheme to highlight the versatile applications of such 3D detectors.

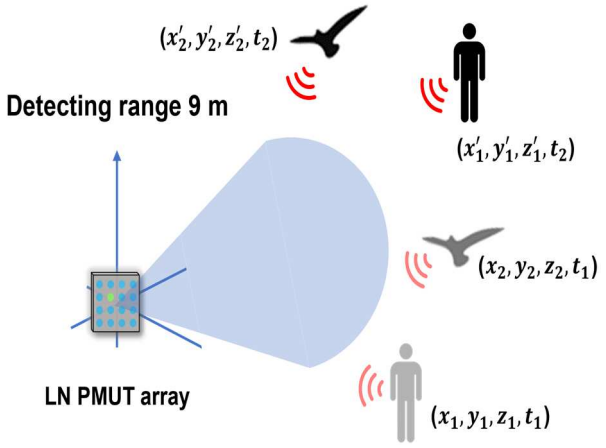

Figure 1: Illustration of the 3D long-range detection system by using a 4×4 lithium niobate PMUT array for a detection distance up to 9 m.

DESIGN AND CHARACTERIZATIONS

In order to improve the electromechanical coupling, the lithium niobate thin film is utilized as the piezoelectric layer for the 3D detector since it has a larger k_t^2 as compared with traditional materials like AlN, PZT and AlScN [11]. **Figure 2a** displays the 4×4 detector system for a total of 16 PMUTs with a pitch distance of 4.6 mm for adjacent units, or λ/2 to avoid the possible grating lobes. During the detection tests, one PMUT at the center of the array is used as the transmitter (T_x, noted as red) and the rest 15 PMUTs are used as the receivers (R_x). The received

signals are processed to reconstruct the detected object through the receiving beamforming scheme. **Figure 2b** shows the cross-section of the single PMUT with an acoustic package. This package is optimized by matching the PMUT acoustic impedance with the medium to improve acoustic energy transmission. The PMUTs array has a very small form factor of only 14.5 mm x 14.5 mm, making it highly compact when compared with conventional ultrasound transducer arrays. An optical photo of the front side of the PMUT array is shown in **Figure 2c**. Each PMUT is aligned with the corresponding opening as shown in the cross-sectional view in **Figure 2b**. **Figure 2d** displays the backside photo of the PMUTs array. A metal lid is used to house the PMUT and direct the acoustic wave spreading from the front opening.

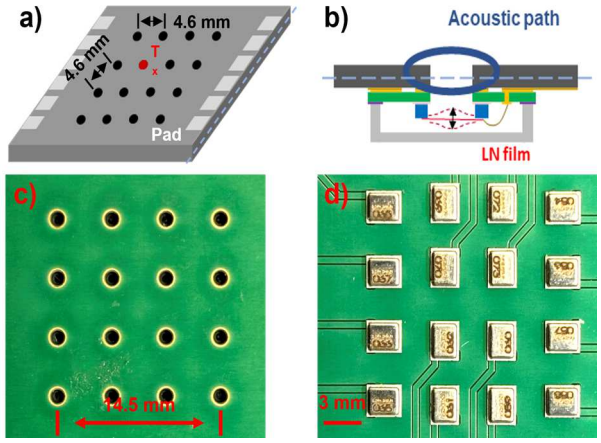

Figure 2: (a) Schematic of the PMUT array board with a pitch size of λ/2 to reduce grating lobes. (b) Cross-section illustration of the package to show the acoustic path. (c) An optical image of the PMUT front side showing the acoustic output holes and the PMUT array is only 14.5 mm by 14.5 mm. (d) An optical image of the PMUT from the backside, a metal lid is used to house the PMUT.

The frequency response and sound pressure of the PMUTs array is characterized by a microphone (Type 4138, Brüel & Kjær Type 4138-L-006). A continuous 10 V_{pp} rectangular wave is applied to the T_x PMUT with different frequencies and the resulting sound pressures are shown in **Figure 3a**. It is observed that there are two peaks between the frequency of interest from 32 kHz to 60 kHz. The first resonance happens at 38.9 kHz with an RMS sound pressure level of 115 dB, which is induced by the optimized acoustic package. The second resonance corresponds to the mechanical resonance of the PMUTs at 50.4 kHz with an RMS peak value of 120 dB. The acoustic package plays two important roles here. First, the additional resonance effectively broadens the bandwidth of the PMUT which facilitate the acoustic energy transfer. In addition, the internal stress control can be quite challenging to construct low-frequency PMUTs and the manufacturing variations can result in the deviation in the resonant frequency. If the PMUT is not operating at its resonant frequency, the transmitting/receiving efficiency will be

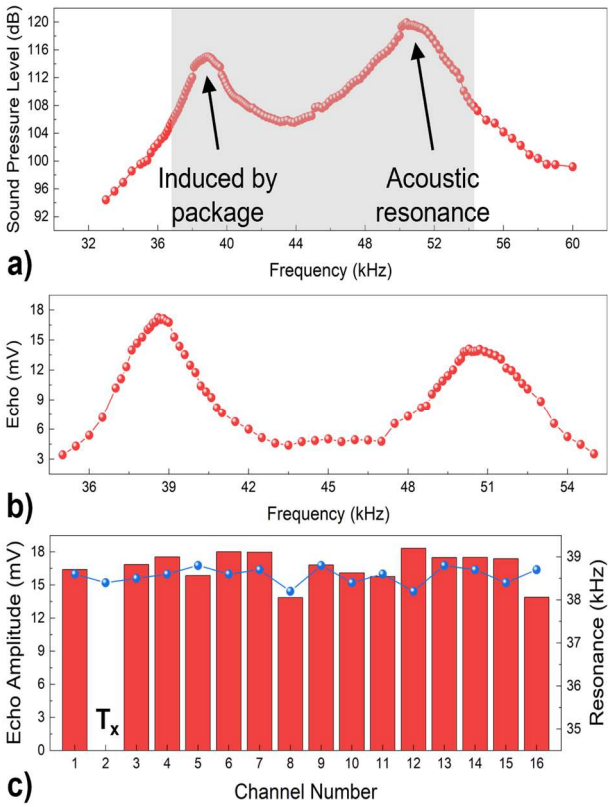

Figure 3: (a) The measured sound pressure level (SPL) of a transmission PMUT (T_x) by a microphone 2 cm away. (b) Pulse-echo voltage vs. frequency measurements at 1 m away. The largest echo amplitude is found at 38.9 kHz. (c) The measured echo amplitude (red columns) and resonant frequency (blue dots) of the 15 receiving PMUTs, where channel 2 is used as the T_x.

significantly lowered. On the other hand, the induced resonance by the acoustic package is relatively easy to control to help align the resonance of all the devices despite of their nonuniformity during the fabrication process. **Figure 3b** shows the characterization results for the pulse-echo frequency responses of the PMUT by measuring the echo reflected by a plate reflector at a distance of 1 m away. A PMUT adjacent to the T_x is used as R_x during this measurement. It can be observed that while a higher sound pressure level is obtained at 50.4 kHz, the echo amplitude reaches a maximum value of 18 mV at the lower resonant frequency resonance at 38.9 kHz. This can be attributed to the low medium attenuation at the low ultrasound frequency at 38.9 kHz and the better resonance alignment of the package. In order to demonstrate the uniformity of the devices, pulse-echo measurement is conducted for all R_x channels under the same conditions and the result is summarized in **Figure 3c.** The resonance frequency of the T_x/R_x pairs is found at 38.5 ± 0.3 kHz and all measured resonant frequencies are within the half-power bandwidth of the T_x PMUT. In terms of echo amplitude, the average echo collected by the 15 Rx channels is 16.65 mV with a variance of 13.4%. This good uniformity ensures the good signal quality and performances for the 3D ultrasonic detector.

DETECTION RESULTS

In order to characterize the range sensing distance, a pulse-echo measurement is conducted at different distances. As shown in **Figure 4a**, a plastic plate facing the PMUTs array is placed 3, 5, 7, and 9 m away during the measurements. The transmitting PMUTs are connected to a function generator and driven by a 10-cycle, 12 V_{pp} (positively biased) signal at 38.4 kHz with a square wave. The 38.4 kHz driving frequency is chosen as the transmitting frequency to best match all R_x channels. The R_x PMUTs are connected to the oscilloscope after being amplified and filtered by a charge amplifier and bandpass filter (passband: 20 kHz to 80 kHz) respectively as shown in **Figure 4b**.

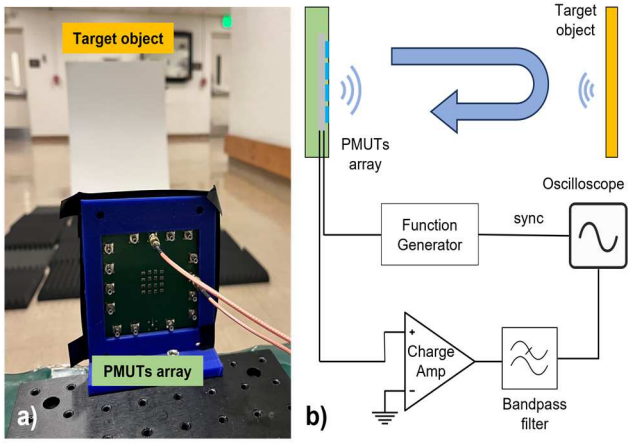

Figure 4: (a) The experimental setup of the range sensing in air. (b) Block diagram of the pulse-echo measurement which is used for range sensing.

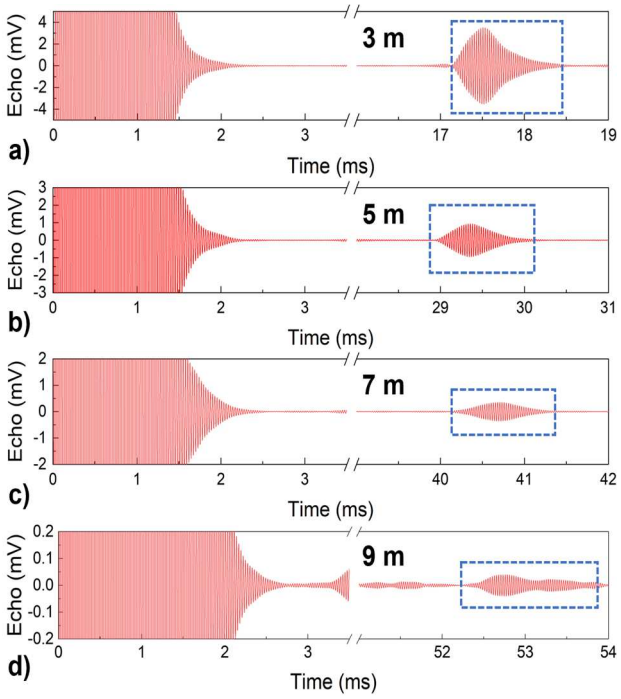

Figure 5: Echo signals received at (a) 3 m, (b) 5 m, (c) 7 m, and (d) 9 m.

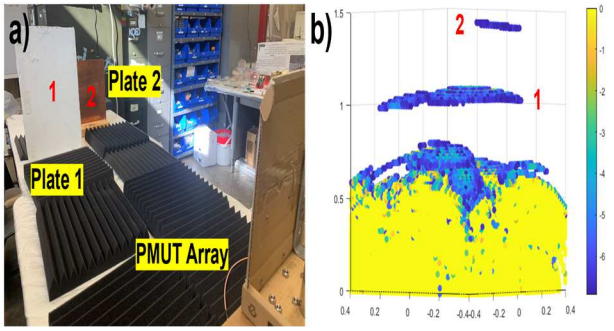

Figure 6: Multiple-object detections. (a) The plastic and metal plate are placed 1 m and 1.5 m away from the PMUT array. (b) Reconstructed 3D imaging results for the two objects.

The collected echoes at different distances are shown in **Figure 5a** to **Figure 5d**. The maximum amplitudes of the echo signals at 3, 5, 7, 9 m are 7.1, 2, 0.77, 0.08 mV respectively. The signals decay as the distance increases due to the attenuation in air [12]. The pulse-echo timing periods can be used to calculate the distances of the plate away from the detection system and the results match well with real values measured by a laser distometer. A robust signal-to-noise ratio (SNR) of over 20 dB is still maintained at 7 m and the largest detection range is 9 m as defined by SNR>10 dB. This is comparable to the state-of-the-art range finder based on PMUT [7].

The capability of multiple-object detection for the PMUTs detector is also demonstrated. As shown in **Figure 6a**, two plates made of different materials are placed in front of the PMUT array at a distance of 1 m and 1.5 m. The echo signals are collected by all the 15 R_x channels separately to reconstruct the 3D image using the delay multiply and sum algorithm. **Figure 6b** displays the reconstructed image where the plastic plate #1 and metal plate #2 can be clearly observed with the well-matched distances. A damping region of around 0.5 m can be observed due to the ring-down and crosstalk between the T_x and R_x elements, which can also be observed in the beginning part of the echo signal in **Figure 5** and this ring down phenomenon could be further reduced by various schemes [13].

Furthermore, we demonstrate the capability of our ultrasonic 3D detector in detecting moving objects. As illustrated in **Figure 7a** to **Figure 7c**, a volunteer moves with cargo from a right 35° to a left 20° angle, mimicking real factory conditions at a distance greater than 3 m. Throughout this movement, the 3D detector continuously gathers echo information and reconstructs the imaging using the same scheme and algorithm detailed in Figure 6. The resulting reconstructed image, displayed in the figure's right part (with the damping region removed for simplicity), reveals the center positions of three moments: (2, -0.3, 2.95), (0.75, -0.4, 3.2), (-1.2, -0.4, 3.25), respectively. These captures align closely with the positions and angles of the object recorded by the distometer. These imaging results validate a field of view exceeding 50° while detection range more than 3 m, which is the longest 3D detection distance reported.

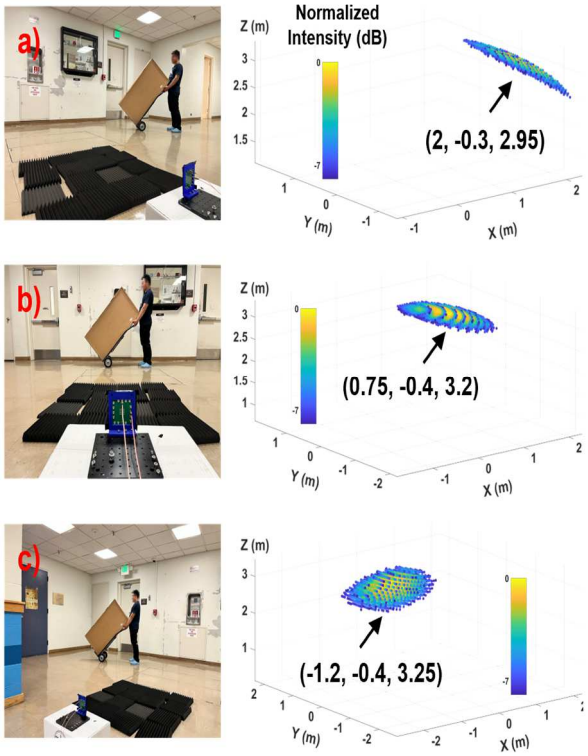

Figure 7: The detection of a moving object at three different moments and at three different positions: at (a) at the right-35° direction and 3.6 m away, (b) at the front-0° direction and 3.3 m away, and (c) at the left-20° direction and 3.5 m away.

CONCLUSION

In this work, we demonstrated a long-range 3D ultrasonic detector based on a 4×4 PMUTs array. Lithium niobate is utilized as the piezoelectric materials for better electromechanical coupling and an acoustic package is designed to mitigate the frequency mismatch during the fabrication process. The second resonance frequency induced by the acoustic package broadens the bandwidth of the PMUT which further facilitates the acoustic energy transfer in air. The prototype PMUT detector manages to detect objects with a distance up to 9 m. In addition, it can also detect multiple objects simultaneously and capture the motions of detected objects with a field of view of over 50°. This detection range is comparable with the state-of-the-art range finder integrated with ASIC without 3D detection. As such, this work shows the longest 3D detections by using PMUTs. The versatile capabilities demonstrated here show the potential of such miniaturized ultrasonic transducers in sensing systems.

ACKNOWLEDGEMENTS

This work is supported by the membership of BSAC (Berkeley Sensor and Actuator Center).

REFERENCES

[1] Yeo, H.S., and Quigley, A., A. "Radar sensing in human-computer interaction", *interactions* 25.1 (2017): 70-73.

[2] Kimoto, K., Asada, N., Mori, T., Hara, Y., and Ohya, A., "Development of small size 3D LIDAR", *2014 IEEE International Conference on Robotics and Automation (ICRA)*. IEEE, 2014.

[3] Przybyla, R.J., Tang, H.Y., Guedes, A., Shelton, S.E., Horsley, D.A., and Boser, B.E., "3D ultrasonic rangefinder on a chip", *IEEE Journal of Solid-State Circuits* 50.1 (2014): 320-334.

[4] Roy, K., Lee, J.E.Y., and Lee, "Thin-film PMUTs: a review of over 40 years of research", *Microsystems & Nanoengineering* 9.1 (2023): 95.

[5] Xia, F., Peng, Y., Pala, S., Arakawa, R., Yue, W., Tsao, P.C., Chen, C.M., Liu, H., Teng, M., Park, J.H., and Lin, L., "High-SPL and Low-Driving-Voltage pMUTs by Sputtered Potassium Sodium Niobate", *2023 IEEE 36th International Conference on Micro Electro Mechanical Systems (MEMS)*. IEEE, 2023.

[6] Luo, G.L., Kusano, Y., and Horsley, D.A., "Airborne piezoelectric micromachined ultrasonic transducers for long-range detection", *Journal of Microelectromechanical Systems* 30.1 (2020): 81-89.

[7] Przybyla, R.J., Shelton, S.E., Lee, C., Eovino, B.E., Chau, Q., Kline, M.H., Izyumin, O.I., and Horsley, D.A., "Mass Produced Micromachined Ultrasonic Time-Of-Flight Sensors Operating in Different Frequency Bands", *2023 IEEE 36th International Conference on Micro Electro Mechanical Systems (MEMS)*. IEEE, 2023: 961-964.

[8] Shao, Z., Pala, S., Peng, Y., and Lin, L., "Bimorph Pinned Piezoelectric Micromachined Ultrasonic Transducers for Space Imaging Applications", *Journal of Microelectromechanical Systems* 30.4 (2021): 650-658.

[9] Shao, Z., Peng, Y., Pala, S., Liang, Y., and Lin, L., "3D Ultrasonic Object Detections with >1 Meter Range", *Proceedings of 34th IEEE Micro Electro Mechanical Systems Conference*, Virtual, Jan. 2021

[10] Sammoura, F., Smyth, K., Kim, S.G., and Lin, L., "An accurate equivalent circuit for the clamped circular multiple-electrode PMUT with residual stress", *2013 IEEE International Ultrasonics Symposium (IUS)*. IEEE, 2013: 275-278.

[11] Pop, F., Herrera, B., and Rinaldi, M., "Lithium Niobate Piezoelectric Micromachined Ultrasonic Transducers for high data-rate intrabody communication", *Nature communications* 13.1 (2022): 1-12.

[12] Magori, V., "Ultrasonic sensors in air", 1994 *Proceedings of IEEE ultrasonics symposium*. Vol. 1. IEEE, 1994: 471-481.

[13] Pala, S., Shao, Z., Peng, Y., and Lin, L., "Improved Ring-Down Time and Axial Resolution of pMUTs via a Phase-Shift Excitation Scheme", in *2021 IEEE 34th International Conference on Micro Electro Mechanical Systems (MEMS)*, Jan. 2021, pp. 390–393

CONTACT

*Y. Peng; +1-510-697-6951; yande_p@berkeley.edu
*H. Liu; +86-13772488986; liuhanx@outlook.com
*C. Chen; +1-929-490-7107;
chunming_chen@berkeley.edu